Time Delay Can Facilitate Coherence in Self-Driven Interacting Particle Systems

Yongzheng Sun,[1,2,*] Wei Lin,[3,†] and Radek Erban[1,‡]

[1]*Mathematical Institute, University of Oxford, Radcliffe Observatory Quarter, Woodstock Road, Oxford OX2 6GG, United Kingdom*

[2]*School of Science, China University of Mining and Technology, Xuzhou 221116, China*

[3]*School of Mathematical Sciences, LMNS and SCMS, Fudan University, Shanghai 200433, China*

Directional switching in a self-propelled particle model with delayed interactions is investigated. It is shown that the average switching time is an increasing function of time delay. The presented results are applied to studying collective animal behaviour. It is argued that self-propelled particle models with time delays can explain the state-dependent diffusion coefficient measured in experiments with locust groups. The theory is further generalized to heterogeneous groups where each individual can respond to its environment with a different time delay.

PACS numbers: 87.18.Gh,05.40.Ca, 87.18.Tt

Collective animal behaviour is often modelled by individual-based (agent-based) models which assume that each individual alters its behaviour according to signals in its neighbourhood [1–8]. Examples include foraging ant colonies [9], swarming locusts [10], schooling fish [11] and flocking birds [12]. Basic self-driven particle models can successfully explain some experimentally observed group-level properties, but additional conjectures have to be hypothesized at the individual-level to fully explain experimental data [13, 14]. In this Letter, we show that interactional time delays, which are present but often neglected in models of collective animal behaviour, can also explain these experimental group-level observations without making further *ad hoc* conjectures about the behaviour of individuals.

Animal groups often make sudden changes in their direction of movement. In some cases a switch in group direction is a response to an external influence, such as the presence of a predator, but experiments with locusts [10] and prawns [13] have shown that directional switching can occur without an abrupt change in the external environment. In these experiments, the animal motion is constrained to movement in a ring-shaped domain. A group then has two possible modes of coherent motion, clockwise and counterclockwise rotation, and switching between these two modes of behaviour can be described as noise-induced transitions in a bistable potential [14, 15]. Group-level behaviour is then described in terms of the Langevin equation for the average velocity U of the group:

$$\mathrm{d}U = F(U)\,\mathrm{d}t + \sqrt{2D(U)}\,\mathrm{d}W, \tag{1}$$

where $F(U)$ and $D(U)$ are drift and diffusion coefficients, respectively, and $\mathrm{d}W$ is white noise. Classical self-driven particle models predict that $D(U)$ is a constant independent of U [10], i.e. $D(U) \equiv$ const. However, detailed analysis of experimental data reveals that group-level fluctuations increase if the system is in the disorded state with no preferred direction of movement (i.e. $D(U)$ has a local maximum around $U \sim 0$) [14]. This observation has been previously captured in generalized self-driven particle models which postulate that each individual responds to loss of its alignment by increasing its own fluctuations [14, 15], i.e. each individual also has as a state-dependent diffusion coefficient. In this Letter, we show that models with time delays does not need to make this conjecture and can also explain the observed behaviour of $D(U)$.

Time delayed models take into account that the interactions between moving individuals are not necessarily instantaneous because of information-processing times [16, 17]. We consider several ways to incorporate time delays into self-driven particle models of collective animal behaviour. We start with the simplest model which uses the same time delay for all individuals. Later, we also study a generalized model in which we assume that the individuals might respond to low local group alignment by increasing the information processing time. Finally, we investigate the influence of random delays on the switching of direction of movement. All considered scenarios are compatible with available experimental data. Moreover, we find that the mean switching time for a group with constant delays is shorter than that of a group with normally distributed delays and longer than that of a group with exponentially distributed delays.

A simple time delay model of experiments in ring-shaped domains [10, 13] can be formulated as follows. We consider a group of N individuals moving along a one-dimensional circle, which we identify with the interval $\Omega = [0, 1)$ with periodic boundary conditions. Each individual is described by its position, $X_i \equiv X_i(t) \in \Omega$, and velocity, $V_i \equiv V_i(t), i = 1, 2, \ldots, N$. The ring-shaped domain has a sufficient width that individuals can pass each other, i.e. one-dimensional modelling implicitly assumes that individuals can cross through each other [10, 14]. Each individual adjusts its behavior according to the behavior of its neighbours, which can be found less than a distance R (the interaction radius) from it. The set of neighbours of the i-th individual at time t is defined as $J_{i,R}(t) = \{j \in \{1, 2, \ldots, N\} \mid \min(d_{ij}(t), 1-d_{ij}(t)) \leq R\}$, where $d_{ij} = |X_i(t) - X_j(t)|$. The time evolution of X_i

and V_i is then given by the following equations:

$$\mathrm{d}X_i = V_i(t)\,\mathrm{d}t, \quad (2)$$

$$\mathrm{d}V_i = \Big[\mathrm{sign}\left(U_{i,R}(t-\tau)\right) - V_i(t)\Big]\mathrm{d}t + \eta\,\mathrm{d}W_i, \quad (3)$$

where $\tau \geq 0$ is the time delay of signal transmission between individuals, $\eta > 0$ is a parameter, $\mathrm{d}W_i$ are standard white noise terms (independently sampled for each individual), $\mathrm{sign} : \mathbb{R} \to \{-1, 0, 1\}$ is the signum function and

$$U_{i,R}(t) \equiv \frac{1}{|J_{i,R}(t)|} \sum_{j \in J_{i,R}(t)} V_j(t) \quad (4)$$

is the average of the velocities of individuals which are within the R-neighbourhood of the i-th individual at time t. The average velocity of the whole group, $U(t)$, which appeared in Eq. (1) can be obtained using (4) provided that R is large enough, i.e. $U(t) = U_{i,R}(t)$ for R larger than 0.5 and arbitrary i and t.

Model (2)–(3) is equivalent to the standard self-propelled particle model of Vicsek [1, 10, 14] for $\tau = 0$, i.e. for the case when interactions between individuals are assumed to occur instantaneously. If $\tau > 0$, then the model takes into account that individuals can only receive and process its neighbour's information after a time delay. Illustrative results computed by model (2)–(3) are presented in Fig. 1(a). We plot the average velocity of the group, $U(t)$, as a function of time for $N = 30$ individuals. The initial positions of individuals are taken uniformly from the interval $[0, 1]$, and the initial velocities are normally distributed numbers with zero mean and unit variance. The presented time series uses different values of time delay τ in different time intervals. We initially report results of the delay-free model ($\tau = 0$) for $t \in [0, 10^3)$. Then we take $\tau = 0.5$ for $t \in [10^3, 2 \times 10^3)$ and $\tau = 1$ for $t \geq 2 \times 10^3$. We can clearly see switching between two states corresponding to clockwise ($U \sim -1$) and counterclockwise ($U \sim 1$) movement of the group. We also conclude that the switching time between different directions of motion increases with increased time delay.

The mean switching time estimated from long time stochastic simulations is plotted in Fig. 1(b) as a function of group size N. As the group size increases the mean switching time is significantly increased. We again compare results computed for the non-delay model ($\tau = 0$) with results computed for the models with delays ($\tau = 0.5$ and $\tau = 1$). The mean switching time is an increasing function of τ for all values of N. This is further illustrated in Fig. 1(c) where we present simulations of model (2)–(3) for different transmission delay times τ for $N = 20$.

To get some insights into the mechanism behind the generation of ordered motion of the self-propelled particle model, we investigate model (2)–(3) where the interaction radius is so large that all individuals interact with

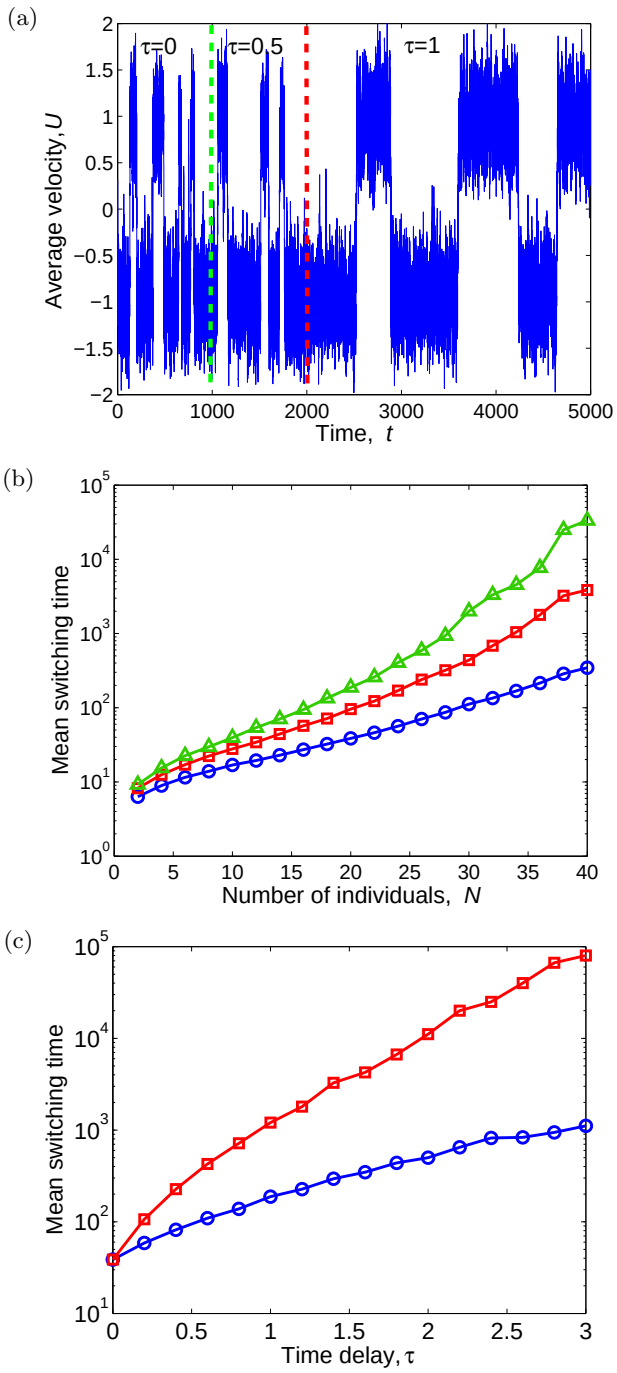

FIG. 1: (color online). (a) *Average velocity $U(t)$ calculated by the model (2)–(3) with $N = 30$, $R = 0.15$, $\eta = 2$. We use $\tau = 0$ for times $t \in [0, 10^3)$, $\tau = 0.5$ for times $t \in [10^3, 2\times10^3)$, and $\tau = 1$ for times $t \geq 2 \times 10^3$.*
(b) *Mean switching time as a function of the size of group N for $\tau = 0$ (blue circles), $\tau = 0.5$ (red squares) and $\tau = 1$ (green triangles). Note the log scale on the y-axis.*
(c) *Mean switching time as a function of the time delay for model (2)–(3) (blue circles) and generalized model (10)–(11) (red squares). Parameter values used are $N = 20$, $R = 0.15$, $\eta = 2$. Note the log scale on the y-axis.*

each other. The local velocity average $U_{i,R}(t)$ in equation (3) is then equal to the global velocity average $U(t)$ and Eq. (3) reduces to

$$\mathrm{d}V_i = \Big[\mathrm{sign}\left(U(t-\tau)\right) - V_i(t)\Big]\mathrm{d}t + \eta\,\mathrm{d}W_i, \qquad (5)$$

which can be further analysed. Adding Eqs. (5) for $i = 1, 2, \ldots, N$, and dividing by N, we obtain delayed stochastic differential equation for $U(t)$

$$\mathrm{d}U = \Big[\mathrm{sign}\left(U(t-\tau)\right) - U(t)\Big]\mathrm{d}t + \eta\, N^{-1/2}\,\mathrm{d}W. \qquad (6)$$

Let $P(u,t)$ denote the probability density of the stochastic process defined by Eq. (6), i.e. $P(u,t)\mathrm{d}u$ is the probability that $U(t) \in [u, u+\mathrm{d}u)$. It satisfies the delay Fokker-Planck equation [18, 19], as discussed in Supplemental Material (SM). Using the small delay approximation method [18, 19], the first order approximation to stationary probability distribution $P_{st}(u) = \lim_{t\to\infty} P(u,t)$ is given by

$$P_{st}(u) \approx C\exp[-\phi(u)], \qquad (7)$$

where C is a normalization constant and the potential $\phi(u)$ is given by

$$\phi(u) = -\frac{2N}{\eta^2}\left[\int^u \mathrm{erf}\left\{\sqrt{\frac{N}{2\eta^2\tau}}[(1-\tau)\nu + \tau\,\mathrm{sign}(\nu)]\right\}\mathrm{d}\nu - \frac{u^2}{2}\right]. \qquad (8)$$

Here, the error function is defined by $\mathrm{erf}(x) = \frac{2}{\sqrt{\pi}}\int_0^x \exp(-z^2)\mathrm{d}z$. The stationary distribution approximation given by (7) has two global maxima at $u = \pm 1$ as shown in Fig. 2. One can clearly distinguish the quasi-stationary states when the transmission delays are large, which is consistent with the simulation results shown in Fig. 1(a).

The above analysis is only valid for large values of R. In the case of the original local interaction model (2)–(3), we will follow the computational approach in [20] to estimate the drift and diffusion coefficients in equation (1) numerically. This approach was previously applied to experimentally measured time series for locust groups [14]. The approximation of the diffusion coefficient $D(u)$ is given by

$$D(u) \approx \frac{1}{2}\left\langle \frac{[U(t+\delta t) - U(t)]^2}{\delta t}\right\rangle\Big|_{U(t)=u}, \qquad (9)$$

where $\langle\cdot\rangle$ denotes an average over many realizations and δt is an effective time scale on which the one-dimensional approximation (1) holds. The estimated diffusion coefficient for the model (2)–(3) with instantaneous interaction (i.e., $\tau = 0$) is approximately constant (see Fig. 1A in [14]). Running long time simulations of delayed model (2)–(3) and using $\delta t = 0.1$ in (9), we present the estimated effective diffusion coefficient in Fig. 3 for $\tau = 1$. Restricting the values of U to $[-1, 1]$, the diffusion coefficient in Fig. 3 has approximately quadratic shape which qualitatively compares well with the analysis of locust experimental data (see Fig. 2A in [14]). In order to mimic the quadratic shape of the diffusion coefficient, Yates *et.al* [14] hypothesized a nontrivial diffusion term for the description of individuals. However, we see from Fig. 3 that the estimated diffusion coefficient of the delayed interaction model (2)–(3) can also explain the experimental observations. Moreover, the diffusion coefficient of model (2)–(3) has a local maximum near $U = 0$, and it has minimal values near $U = \pm 1$. Consequently, noise regains its strength as the system leaves $U = \pm 1$ which helps

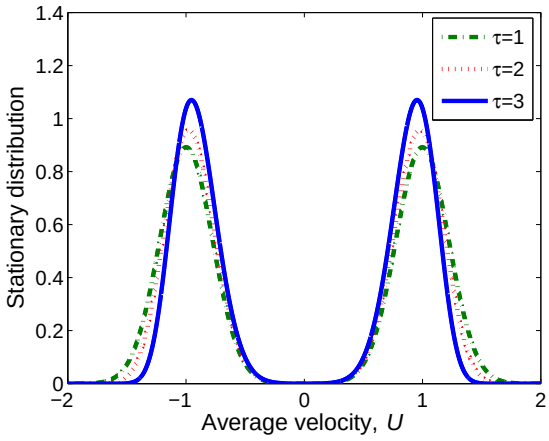

FIG. 2: (color online). *The approximation of stationary distribution given by* (7) *for parameters* $N = 20$, $\eta = 2$ *and* $\tau = 1$ *(dash-dot line),* $\tau = 2$ *(dotted line),* $\tau = 3$ *(solid line).*

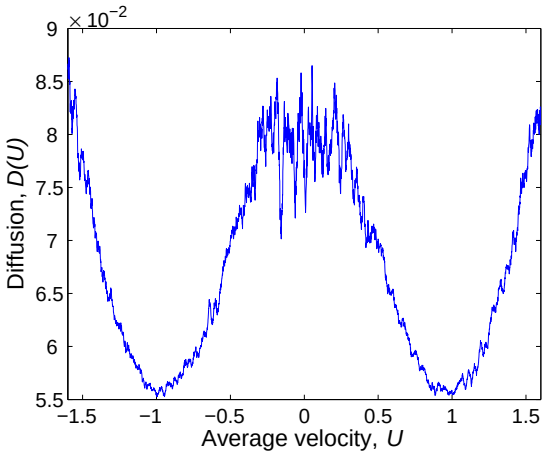

FIG. 3: (color online). *Estimation of the diffusion coefficient of the local interaction model* (2)–(3) *with* $N = 30, R = 0.15, \eta = 2$ and $\tau = 1$. *The diffusion coefficient is estimated by using (9) with* $\delta t = 0.1$.

the system to return into one of the favourable states $U = \pm 1$. The estimated drift coefficient, effective potential, and the stationary probability for model (2)–(3) are presented in SM (see Figs. S1 and S2) together with the computational analysis which justifies the validity of the one-dimensional group-level description given by Eq. (1).

Model (2)-(3) assumes that all interactions occur with the same time delay. However, actual delays in real systems may not necessarily be the same for all individuals in the system. Delays might also be state dependent because disordered states (confusion) might increase the length of the information transmission delay. To take these effects into account, we generalize model (2)-(3) by replacing Eq. (3) with

$$\mathrm{d}V_i = \Big[\mathrm{sign}\left(U_{i,R}(t-\tau_i)\right) - V_i(t)\Big]\mathrm{d}t + \eta\,\mathrm{d}W_i, \qquad (10)$$

i.e. each individual has its own time delay τ_i, $i = 1, 2, \ldots, N$. First, we assume that $\tau_i \equiv \tau_i(t)$ depends on time t as follows:

$$\tau_i(t) = \tau\{1 + [\max_{j\in J_{i,R}}(|V_j(t)|) - |U_{i,R}(t)|]\}, \qquad (11)$$

where τ is a constant corresponding to the information transmission delay in high local group alignment, $\max_{j\in J_{i,R}}(|V_j(t)|)$ is the maximum absolute value of the velocity of the neighbours of individual i at time t. Equation (11) means that the information transmission delay will increase when the local group alignment is low. This assumption on the delay is satisfied in real traffic flow. For instance, it will need longer time for a driver to recognize signals and make responses in traffic jams than in good traffic conditions [21].

The mean switching time of the original model (2)–(3) and the generalized model (10)–(11) as a function of the scale of time delay τ for a specific case of the group size ($N = 20$) is shown in Fig. 1(c). The mean switching time is significantly increased for all values of τ in comparison with the original model which demonstrates that moving individuals can keep a high aligned state by increasing their response time when the group looses its coherence. The mean switching time as a function of N and the estimated diffusion and drift coefficients are plotted in SM (see Figs. S3 and S4).

In our final example, we consider that time delays τ_i in (10) are constant in time, but different for each individual. The time delays $\tau_i > 0$ are chosen according to distribution $f \equiv f(\tau') : [0, \infty) \to [0, \infty)$ with mean delay $\tau > 0$. We consider random delays τ_i given by the following two different distributions: (i) exponential distribution, i.e. $\tau_i = \zeta(\tau)$, where ζ is exponentially distributed with mean τ; (ii) (truncated) normal distribution: $\tau_i = \tau + c\xi$, where ξ is normally distributed with zero mean and standard deviation one. The delays are constant ($\tau_i = \tau$) for $c = 0$ and are normally distributed around τ for $c \neq 0$ (depending on τ and c the distribution has to be truncated to avoid negative delays and the truncated distribution shifted to keep its mean value equal to τ [22]).

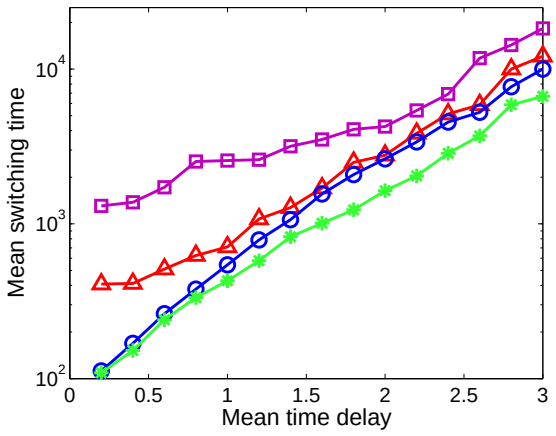

FIG. 4: (color online). *The mean switching time for delays that are normally distributed with $c = 1$ (red triangles), normally distributed with $c = 2$ (magenta squares) and exponentially distributed (green stars) as a function of the scale of the mean time delay. The corresponding results computed with constant delays are plotted as blue circles. The other parameters are $N = 100$, $R = 0.15$ and $\eta = 4$. Note the log scale on the y-axis.*

We compare the mean switching time for distributed delays with the original model (constant delay) in Fig. 4. We again see increased coherence as the average time delay τ increases. It can be observed that the average switching time for standard normally distributed delays is longer than that for constant delays. However, the average switching time for exponentially distributed delays is shorter than that for constant delays. The mean switching time for normally distributed delays with $c = 2$ is significantly increased for all values of τ in comparison with the mean switching time for normally distributed delays with $c = 1$, which implies that, for normally distributed delays, the average switching time increases as the randomness of the delay increases.

To summarize, we have studied the directional switching of a self-driven particle model with constant, time-varying and random delay times, respectively. The presented analytical and numerical results have demonstrated that time delays can significantly influence the group-level dynamics. A rapid transition occurs from disordered movement of individuals within the group to highly aligned collective motion as the density of group or the time delays increase. Moreover, we have reported that the heterogeneity of the group (distribution of time delays) can further facilitate coherence in collective swarm motion.

Acknowledgements: Y. Sun acknowledges financial support from the China Scholarship Council (Grant No. 201308320087). The research leading to these results has received funding from the European Research Council under the *European Community's* Seventh Framework Programme *(FP7/2007-2013)* / ERC *grant agreement* No. 239870. R. Erban would also like to thank the Royal Society for a University Research Fellowship; Brasenose College, University of Oxford, for a Nicholas Kurti Junior Fellowship; and the Leverhulme Trust for a Philip Leverhulme Prize. W. Lin was supported under NNSF of China (Grant No. 11322111).

* Electronic address: suny@maths.ox.ac.uk
† Electronic address: wlin@fudan.edu.cn
‡ Electronic address: erban@maths.ox.ac.uk

[1] T. Vicsek, A. Czirok, E. Ben-Jacob, I. Cohen, and O. Shochet, Phys. Rev. Lett. **75**, 1226 (1995).
[2] I. D. Couzin, J. Krause, N. R. Franks, and S. A. Levin, Proc. Natl. Acad. Sci. U.S.A. **433**, 513 (2005).
[3] C. M. Topaz, A. L. Bertozzi, and M. A. Lewis, Bull. Math. Bio. **68**, 1601 (2006).
[4] W. Yu, G. Chen, and M. Cao, Sys. Control Lett. **59**, 552 (2010).
[5] P. Degond, A. Frouvelle, and J. G. Liu, J. Nonlinear Sci. **23**, 427 (2013).
[6] K. R. Pilkiewicz and J. D. Eaves, Phys. Rev. E. **89**, 012718 (2014).
[7] J.-B. Caussin, A. Solon, A. Peshkov, H. Chaté, T. Dauxois, J. Tailleur, V. Vitelli, and D. Bartolo, Phys. Rev. Lett. **112**, 148102 (2014).
[8] T. Vicsek and A. Zafeiris, Physics Reports **517**, 71 (2012).
[9] T. Biancalani, L. Dyson, and A. J. McKane, Phys. Rev. Lett. **112**, 038101 (2014).
[10] J. Buhl, D. J. T. Sumpter, I. D. Couiz, J. J. Hale, E. Despland, E. R. Miller, and S. J. Simpson, Science **312**, 1402 (2006).
[11] Y. Katza, K. Tunstrøma, C. C. Ioannoua, C. Huepeb, and I. D. Couzin, Proc. Natl. Acad. Sci. U.S.A. **108**, 18720 (2011).
[12] F. Cucker and S. Smale, IEEE Trans. Automat. Control **52**, 852 (2007).
[13] R. P. Mann, A. Perna, D. Strömbom, R. Garnett, J. E. Herbert-Read, D. J. T. Sumper, and A. J. W. Ward, PLOS Computa. Biol. **9**, e1002961 (2013).
[14] C. Yates, R. Erban, C. Escudero, I. D. Couzin, J. Buhl, I. Kevrekidis, P. Maini, and D. Sumpter, Proc. Natl. Acad. Sci. U.S.A. **106**, 5464 (2009).
[15] R. Erban and J. Haskovec, Kinetic and Related Models **5**, 817 (2012).
[16] C. Masoller and A. C. Martí, Phys. Rev. Lett. **94**, 134102 (2005).
[17] L. Mier-y-Teran-Romero, E. Forgoston, and I. B. Schwartz, IEEE Trans. on Robotics **28**, 1034 (2012).
[18] T. D. Frank, Phys. Rev. E **72**, 011112 (2005).
[19] See Supplemental Material for the Fokker-Planck equation and for the derivation of the result given in Eq. (8).
[20] R. Erban, I. G. Kevrekidis, D. Adalsteinsson, and T. C. Elston, J. Chem. Phys. **124**, 084106 (2006).
[21] R. Sipahi and S.-I. Niculescu, in Deterministic Time-Delayed Traffic Flow Models: A Survey (Springer-Verlag, Berlin, 2010).
[22] C. P. Robert, Statistics and Computing, **5**, 121 (1995).